

**Electronic Supplementary Information (ESI)**

**Nonaqueous arylated quinone catholytes for lithium-organic flow batteries**

Dong-Seon Shin,<sup>a</sup> Minjoon Park,<sup>ab</sup> Jaechan Ryu,<sup>a</sup> Inchan Hwang,<sup>a</sup> Jeong Kon Seo,<sup>c</sup> Kwanyong Seo,<sup>\*a</sup> Jaephil Cho<sup>\*a</sup> and Sung You Hong<sup>\*a</sup>

*<sup>a</sup>School of Energy and Chemical Engineering, Ulsan National Institute of Science and Technology (UNIST), 50 UNIST-gil, Ulsan 44919, Republic of Korea. E-mail: kseo@unist.ac.kr; jpcho@unist.ac.kr; syhong@unist.ac.kr*

*<sup>b</sup>Present address: Harvard John A. Paulson School of Engineering and Applied Science, 29 Oxford Street, Cambridge, MA 02138, USA*

*<sup>c</sup>UNIST Central Research Facilities (UCRF), Ulsan National Institute of Science and Technology (UNIST), 50 UNIST-gil, Ulsan 44919, Republic of Korea*

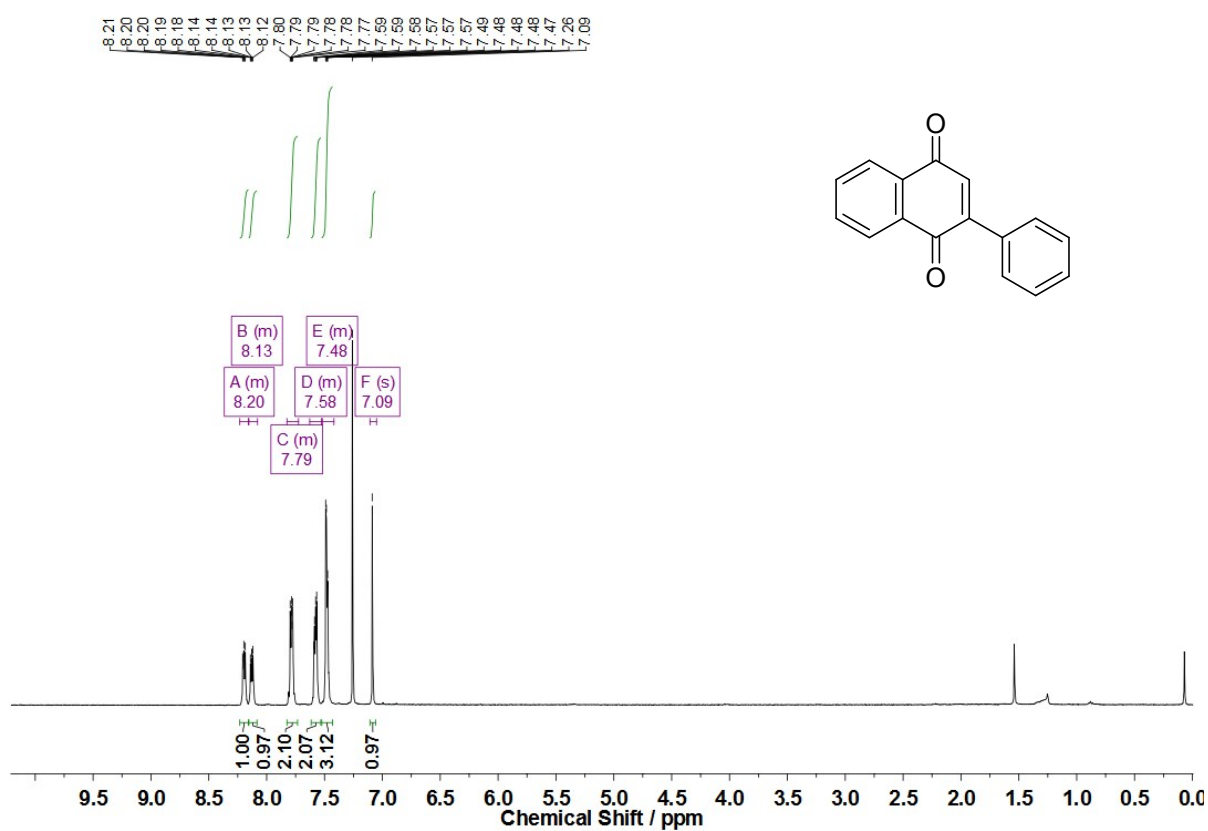
## **Table of contents**

<b>I. General</b> .....	S2
<b>II. Characterization and electrochemical tests</b> .....	S3
<b>III. References</b> .....	S22

### **I. General**

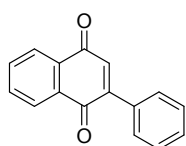
All chemicals were purchased from standard suppliers and used without further purification. Reactions were monitored by thin-layer chromatography (TLC) using Merck silica gel 60F254 glass plate with 0.25 mm thickness. Flash column chromatography was carried out using Merck silica gel 60 (size range: 0.040–0.063 mm). Proton ( $^1\text{H}$ ), carbon ( $^{13}\text{C}$ ), and fluorine ( $^{19}\text{F}$ ) nuclear magnetic resonance (NMR) spectra were recorded on a Bruker AVANCE III HD spectrometer. Chemical shifts are given on the  $\delta$ -scale in ppm. High-resolution mass spectrometry (HRMS) data were measured on a Thermo Scientific Q Exactive Plus Hybrid Quadrupole-Orbitrap mass spectrometer. SEM images were obtained using a FE-SEM (S-4800, Hitachi) operating at 10 kV. A battery cycler (WBC3000, WonAtech) was used to evaluate the electrochemical properties. Cyclic voltammograms and electrochemical impedance spectroscopy (EIS) data were recorded using a VSP-300 multipotentiostat (BioLogic Science Instruments). UV/Vis spectra were recorded on a UV-1800 (Shimadzu). The photocharging experiments were tested using an Oriel Sol3A Class AAA solar simulator.

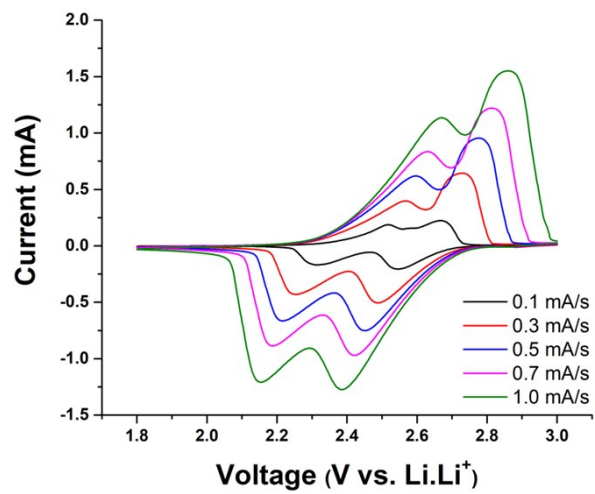
## II. Characterization and electrochemical tests



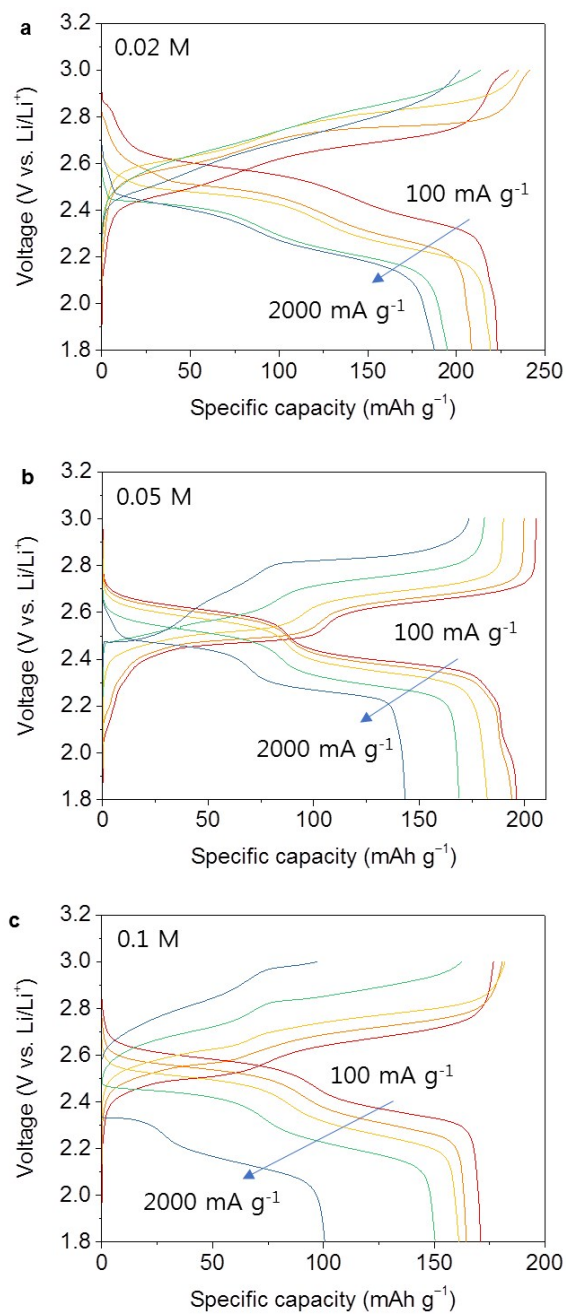
**Fig. S1**  $^1\text{H}$  NMR (400 MHz,  $\text{CDCl}_3$ ) spectrum of PNQ-1.

2-Phenyl-1,4-naphthoquinone (PNQ-1)<sup>S1</sup>: A yellow solid purified by flash column chromatography (n-hexane:ethyl acetate = 20:1).  $R_f$  0.6 (n-hexane:ethyl acetate = 4:1).  $^1\text{H}$  NMR (400 MHz,  $\text{CDCl}_3$ )  $\delta_{\text{H}}$  8.23–8.17 (m, 1H), 8.16–8.08 (m, 1H), 7.82–7.72 (m, 2H), 7.63–7.53 (m, 2H), 7.52–7.42 (m, 3H), 7.09 (s, 1H).

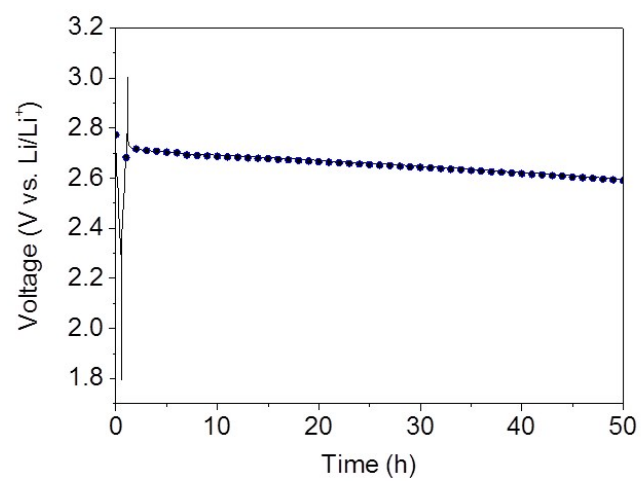




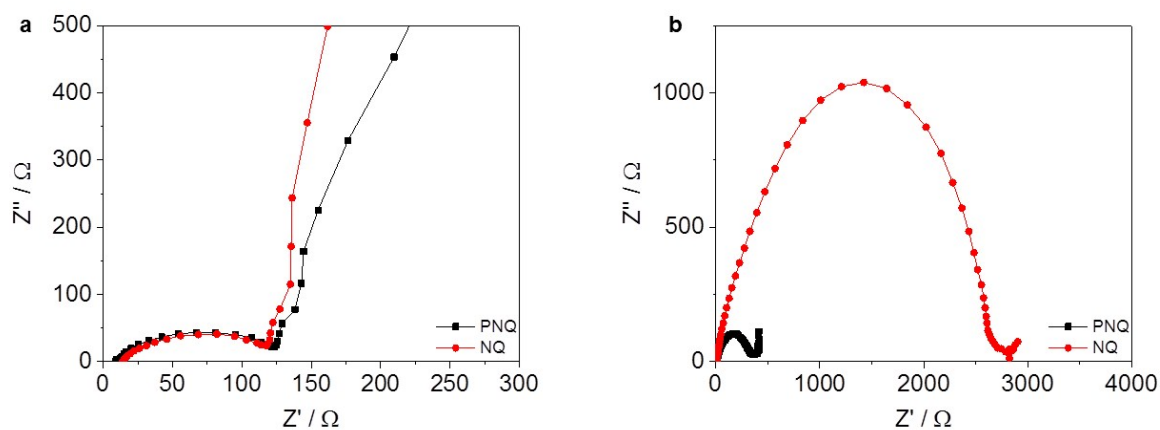
**Fig. S2** Cyclic voltammograms of PNQ-1 within a scan rate range of 0.1–1.0 mV s<sup>-1</sup>.



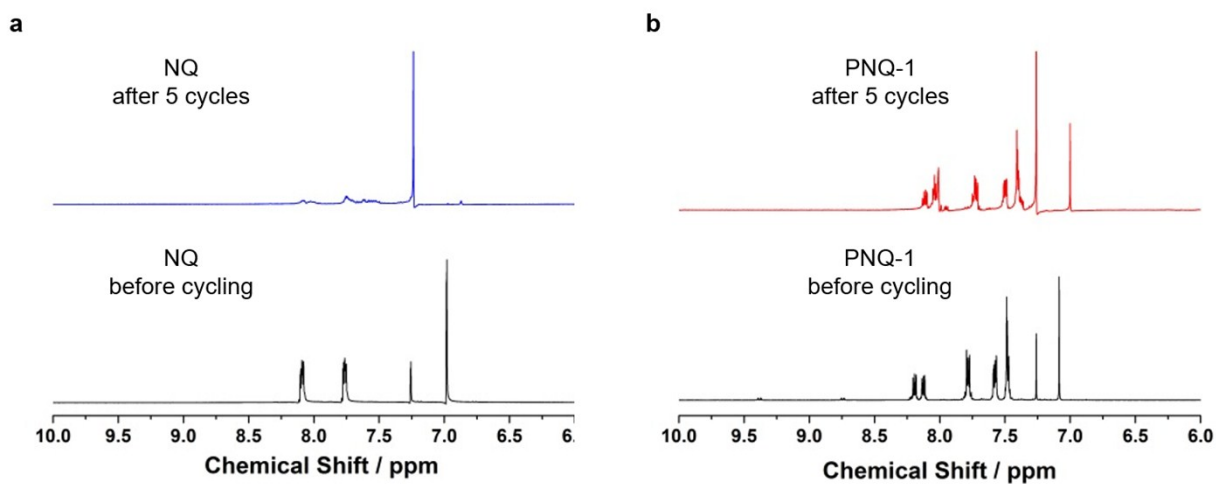
**Fig. S3** Rate capability tests of the PNQ-1 catholyte. (a) 0.02 M, (b) 0.05 M, and (c) 0.1 M of the PNQ-1 catholyte at different current densities: 100, 200, 400, 1000, and 2000 mA g<sup>-1</sup>.



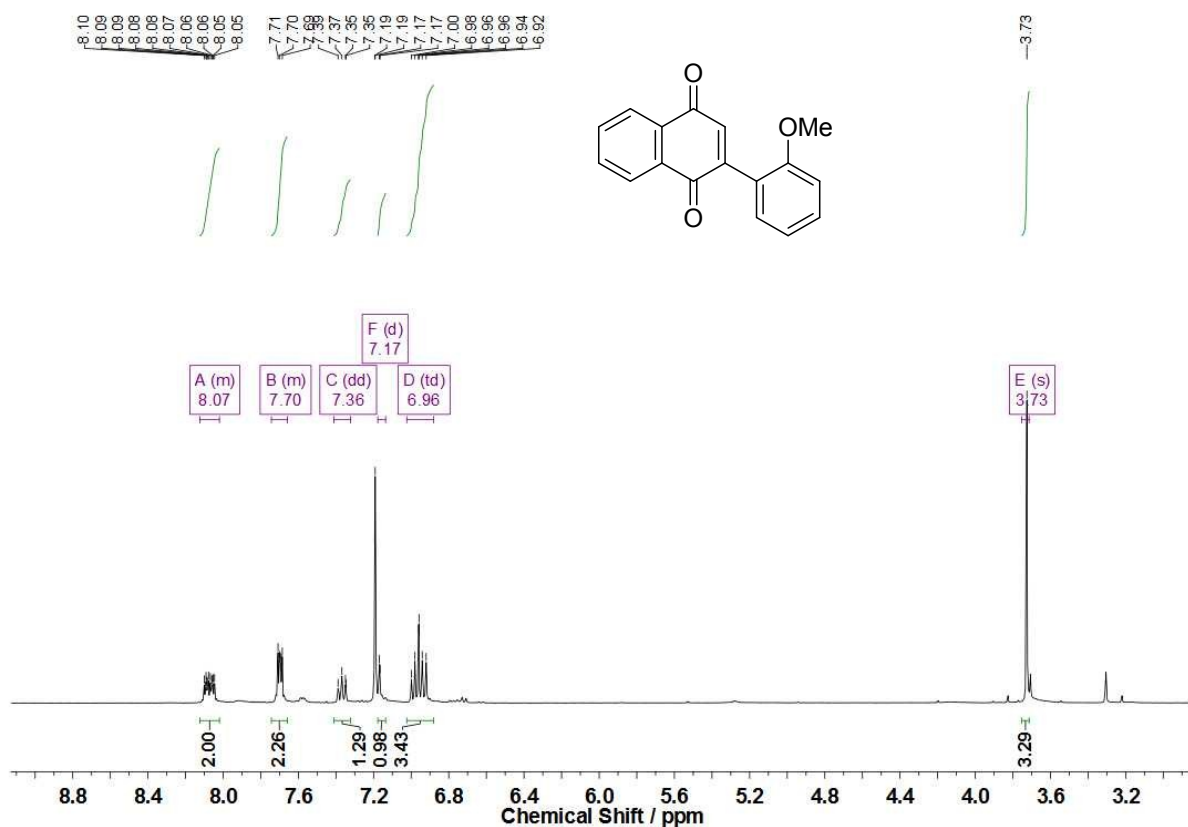
**Fig. S4** The voltage decay profile of the PNQ-1 catholyte after cycling (charged to 3.0 V) at 25 °C.



**Fig. S5** EIS measurements of the NQ and PNQ-1 catholytes (a) at the pristine stage and (b) after 100 cycles. Conditions: After imposing a high current density of  $400 \text{ mA g}^{-1}$  on the cells containing the NQ and PNQ-1 catholytes, the EIS measurements have been carried out by applying an alternating voltage of  $1 \text{ mV}$  over the frequency range from  $10^{-2}$  to  $10^4 \text{ Hz}$ .

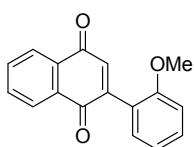


**Fig. S6**  $^1\text{H NMR}$  (400 MHz,  $\text{CDCl}_3$ ) spectra of (a) NQ and (b) PNQ-1 for initial five cycles.



**Fig. S7**  $^1\text{H}$  NMR (400 MHz,  $\text{CDCl}_3$ ) spectrum of PNQ-2.

2-(2-Methoxyphenyl)-1,4-naphthoquinone (PNQ-2)<sup>S2</sup>: A yellow solid purified by flash column chromatography (n-hexane:ethyl acetate = 20:1).  $R_f$  0.5 (n-hexane:ethyl acetate = 4: 1).  $^1\text{H}$  NMR (400 MHz,  $\text{CDCl}_3$ )  $\delta_{\text{H}}$  8.12 – 8.02 (m, 2H), 7.74 – 7.66 (m, 2H), 7.36 (dd,  $J = 12.5, 4.9$  Hz, 1H), 7.17 (d,  $J = 1.5$  Hz, 1H), 6.96 (m, 3H), 3.73 (s, 3H).



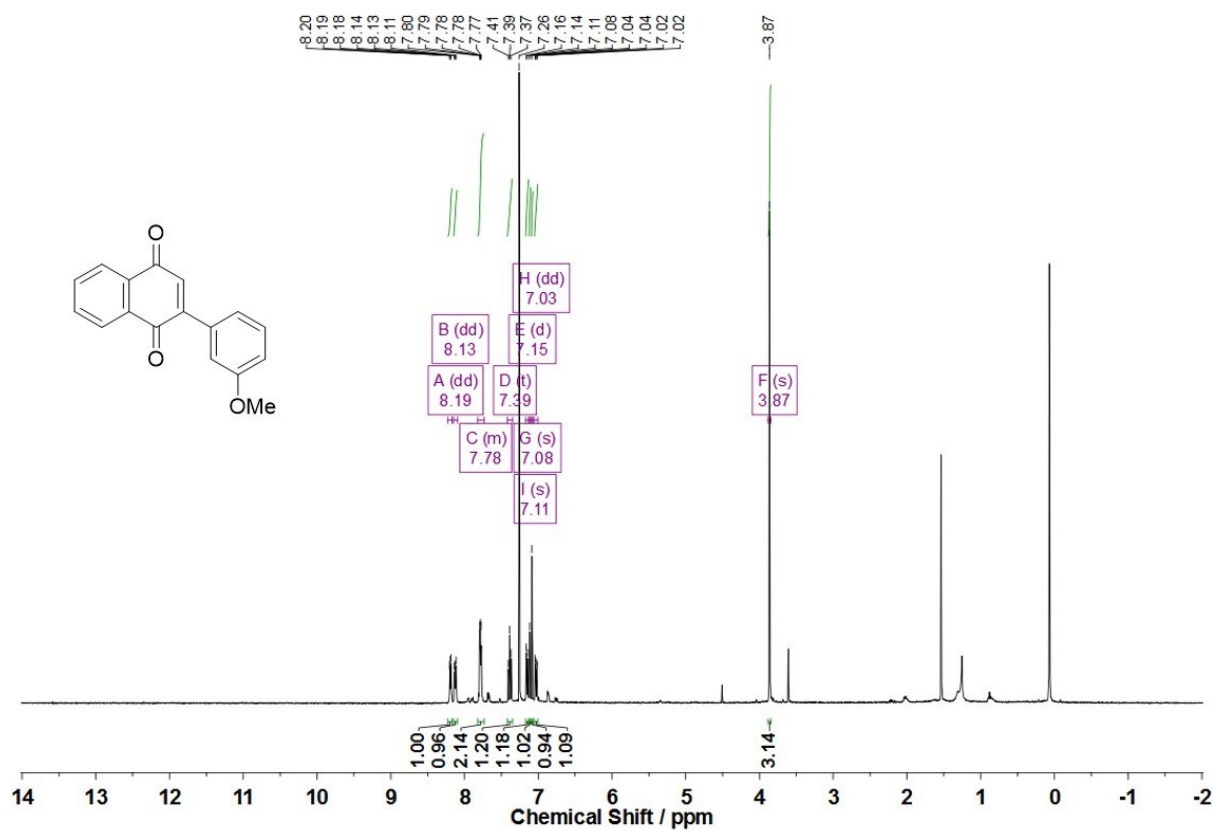
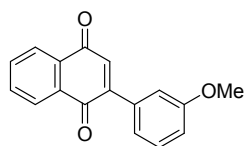


**Fig. S8**  $^1\text{H}$  NMR (400 MHz,  $\text{CDCl}_3$ ) spectrum of PNQ-3.

2-(3-Methoxyphenyl)-1,4-naphthoquinone (PNQ-3)<sup>S3</sup>: A yellow solid purified by flash column chromatography (n-hexane:ethyl acetate = 20:1).  $R_f$  0.5 (n-hexane:ethyl acetate = 4:1).



$^1\text{H}$  NMR (400 MHz,  $\text{CDCl}_3$ )  $\delta_{\text{H}}$  8.19 (dd,  $J = 5.9, 3.2$  Hz, 1H), 8.13 (dd,  $J = 5.9, 3.2$  Hz, 1H), 7.82 – 7.74 (m, 2H), 7.39 (t,  $J = 8.0$  Hz, 1H), 7.15 (d,  $J = 8.5$  Hz, 1H), 7.11 (s, 1H), 7.08 (s, 1H), 7.03 (dd,  $J = 8.3, 2.5$  Hz,

1H), 3.87 (s, 3H).

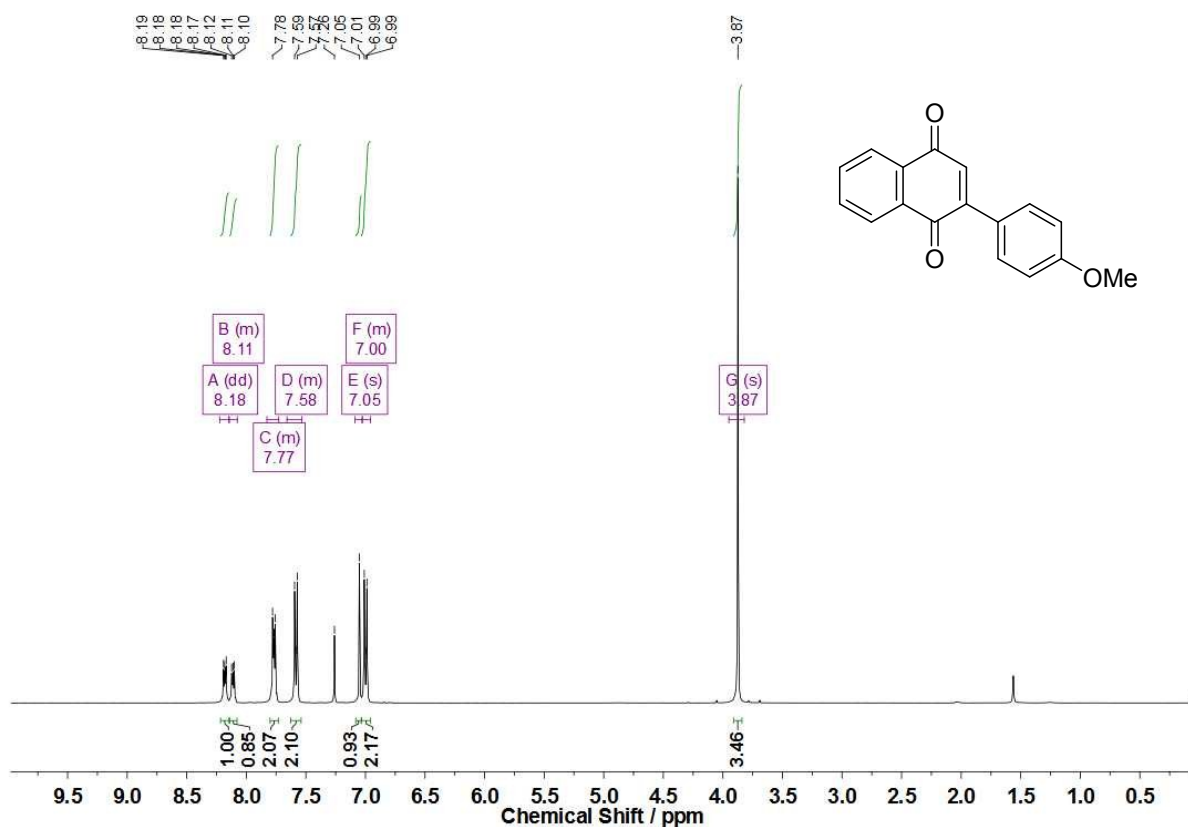
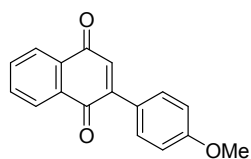


**Fig. S9**  $^1\text{H}$  NMR (400 MHz,  $\text{CDCl}_3$ ) spectrum of PNQ-4.

2-(4-Methoxyphenyl)-1,4-naphthoquinone (PNQ-4)<sup>S3</sup>: A yellow solid purified by flash column chromatography (n-hexane:ethyl acetate = 20:1).  $R_f$  0.5 (n-hexane:ethyl acetate = 4:1).  $^1\text{H}$  NMR (400 MHz,  $\text{CDCl}_3$ )  $\delta_{\text{H}}$  8.20–8.15



(m, 1H), 8.13–8.08 (m, 1H), 7.77 (dd,  $J = 5.0, 3.9$  Hz, 2H), 7.58 (d,  $J = 8.6$  Hz, 2H), 7.05 (s, 1H), 7.00 (d,  $J = 8.7$  Hz, 2H), 3.87 (s, 3H).

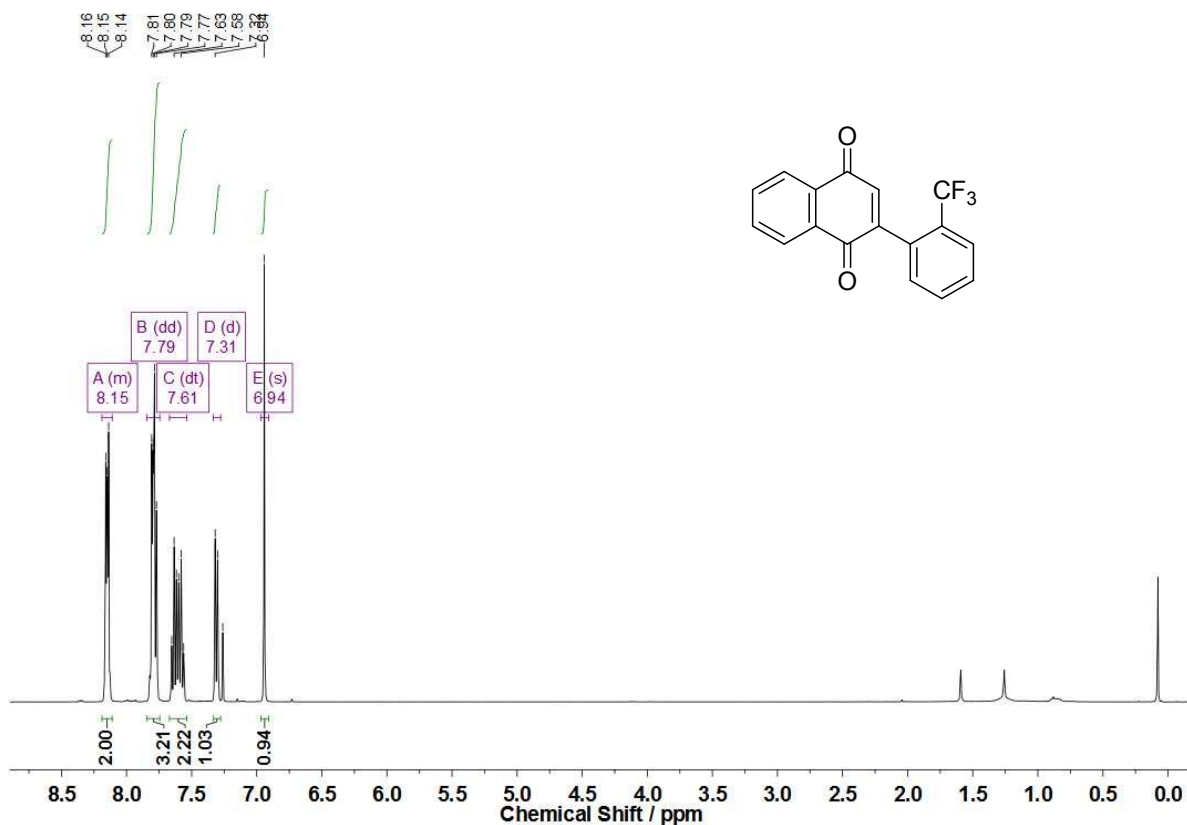


**Fig. S10**  $^1\text{H}$  NMR (400 MHz,  $\text{CDCl}_3$ ) spectrum of PNQ-5.

2-(2-Trifluoromethylphenyl)-1,4-naphthoquinone (PNQ-5): A yellow solid purified by flash column chromatography (n-hexane : ethyl acetate = 20 : 1).  $R_f$  0.4 (n-hexane : ethyl acetate = 4 : 1).  $^1\text{H}$  NMR (400 MHz,  $\text{CDCl}_3$ )  $\delta_{\text{H}}$  8.21 – 8.11 (m, 2H), 7.84 – 7.75 (m, 3H), 7.66 – 7.55 (m, 2H), 7.35 – 7.28 (m, 1H), 6.94 (s, 1H);  $^{13}\text{C}$  NMR (100 MHz,  $\text{CDCl}_3$ )  $\delta_{\text{C}}$  184.61, 148.42, 136.71, 134.11, 134.07, 132.09, 131.85, 131.57, 130.59, 129.29, 127.06, 126.49, 126.32, 99.99;  $^{19}\text{F}$  NMR (376 MHz,  $\text{CDCl}_3$ )  $\delta_{\text{F}}$  -57.96; HRMS-ESI:  $m/z$   $[\text{M}+\text{H}]^+$  calcd for  $\text{C}_{17}\text{H}_{10}\text{F}_3\text{O}_2$ : 303.0633; found: 303.0625.

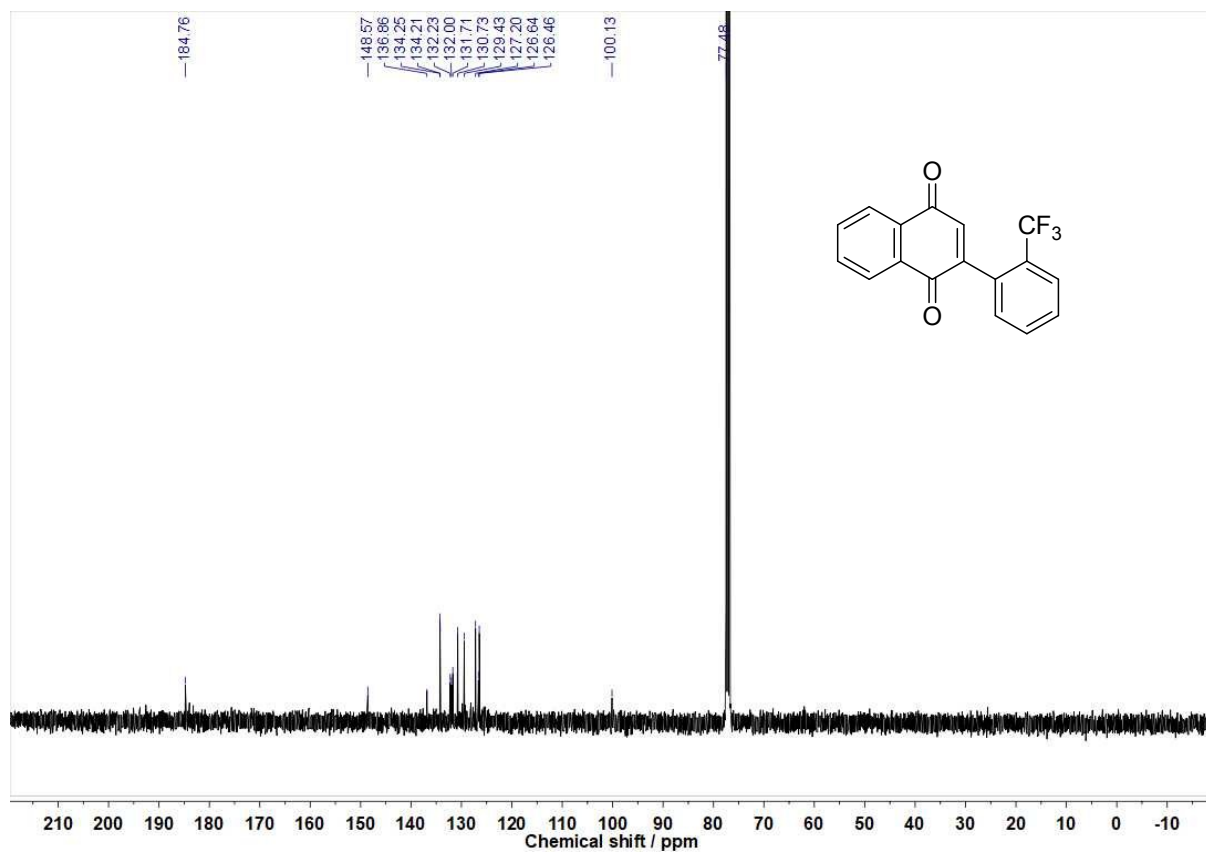


**Fig. S11** <sup>13</sup>C NMR (100 MHz, CDCl<sub>3</sub>) spectrum of PNQ-5.

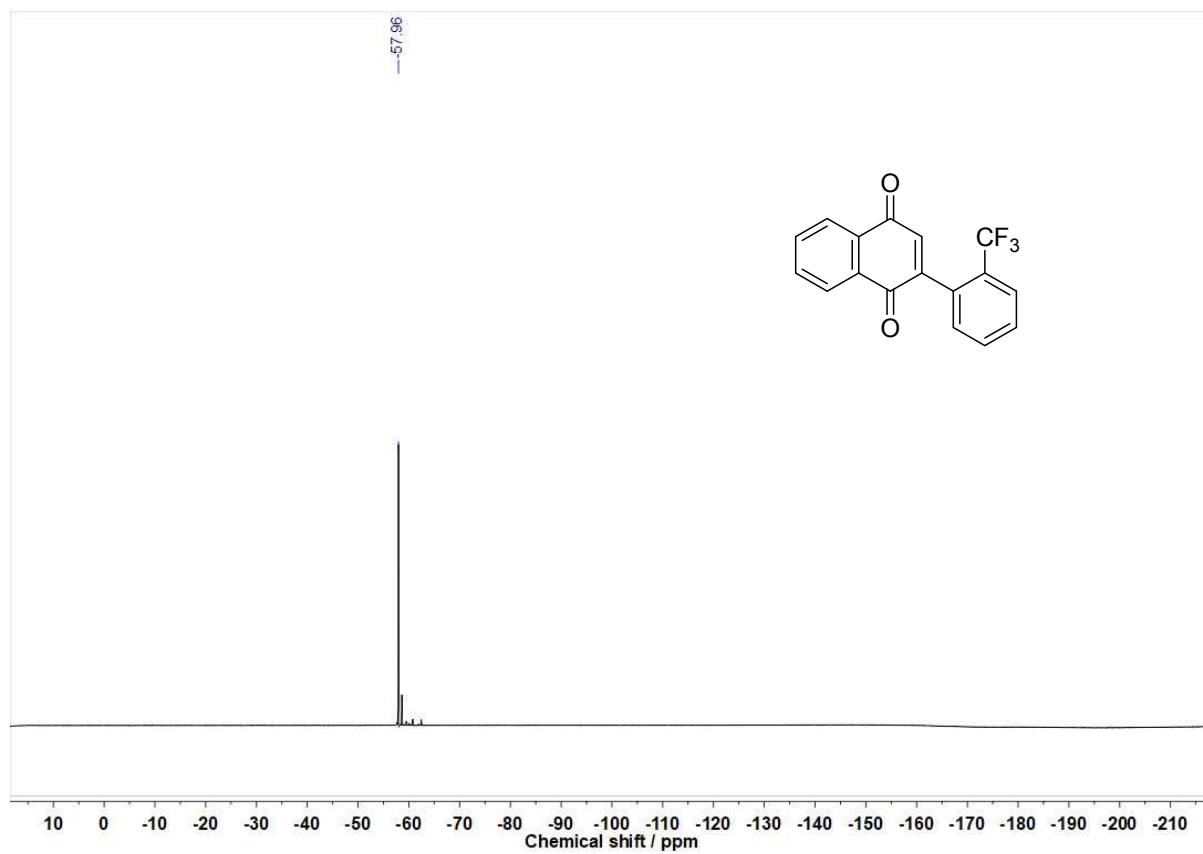


**Fig. S12**  $^{19}\text{F}$  NMR (376 MHz,  $\text{CDCl}_3$ ) spectrum of PNQ-5.

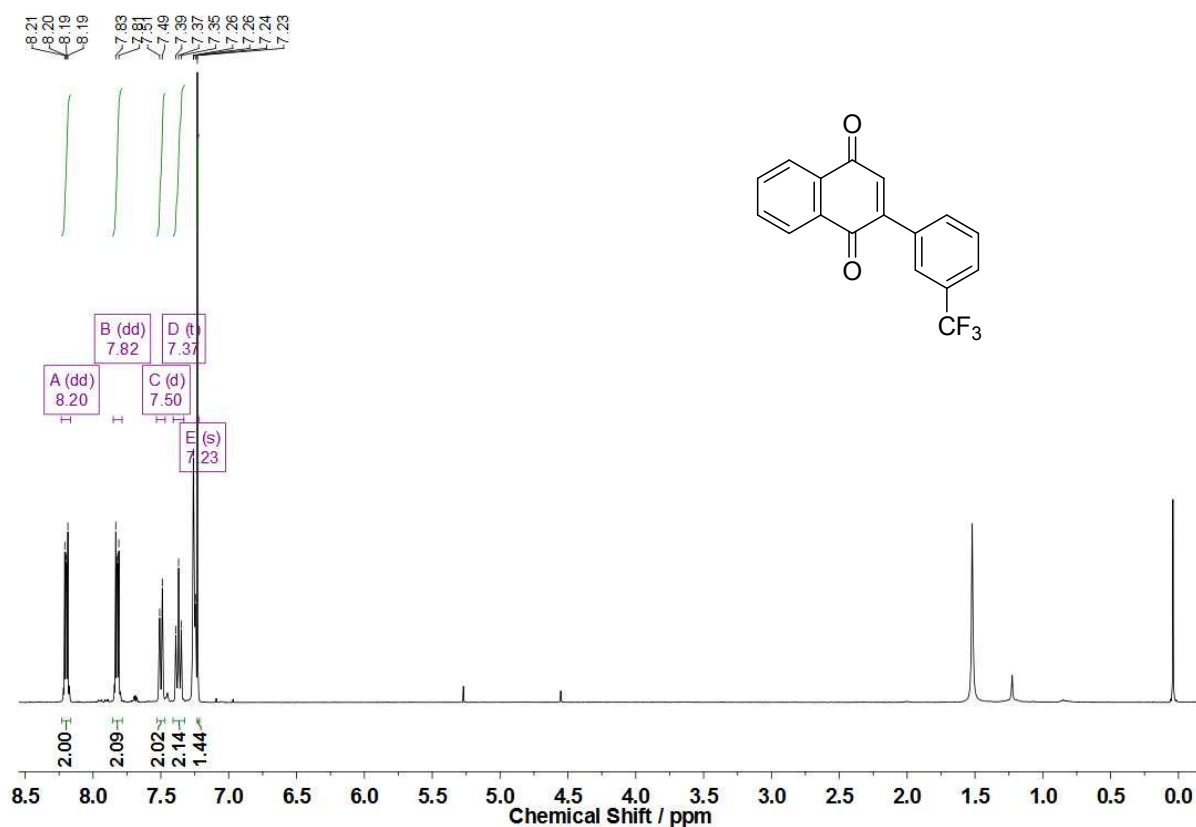
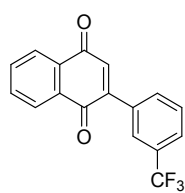


**Fig. S13**  $^1\text{H}$  NMR (400 MHz,  $\text{CDCl}_3$ ) spectrum of PNQ-6.

2-(3-Trifluoromethylphenyl)-1,4-naphthoquinone (PNQ-6)<sup>S3</sup>: A yellow solid purified by flash



column chromatography (n-hexane : ethyl acetate = 20 : 1).  $R_f$  0.4 (n-hexane : ethyl acetate = 4 : 1).  $^1\text{H}$  NMR (400 MHz,  $\text{CDCl}_3$ )  $\delta_{\text{H}}$  8.20 (dd,  $J = 5.8, 3.3$  Hz, 1H), 7.82 (dd,  $J = 5.8, 3.3$  Hz, 1H), 7.50 (d,  $J = 7.8$  Hz, 1H), 7.37 (t,  $J = 8.0$  Hz, 1H), 7.23 (s, 1H).

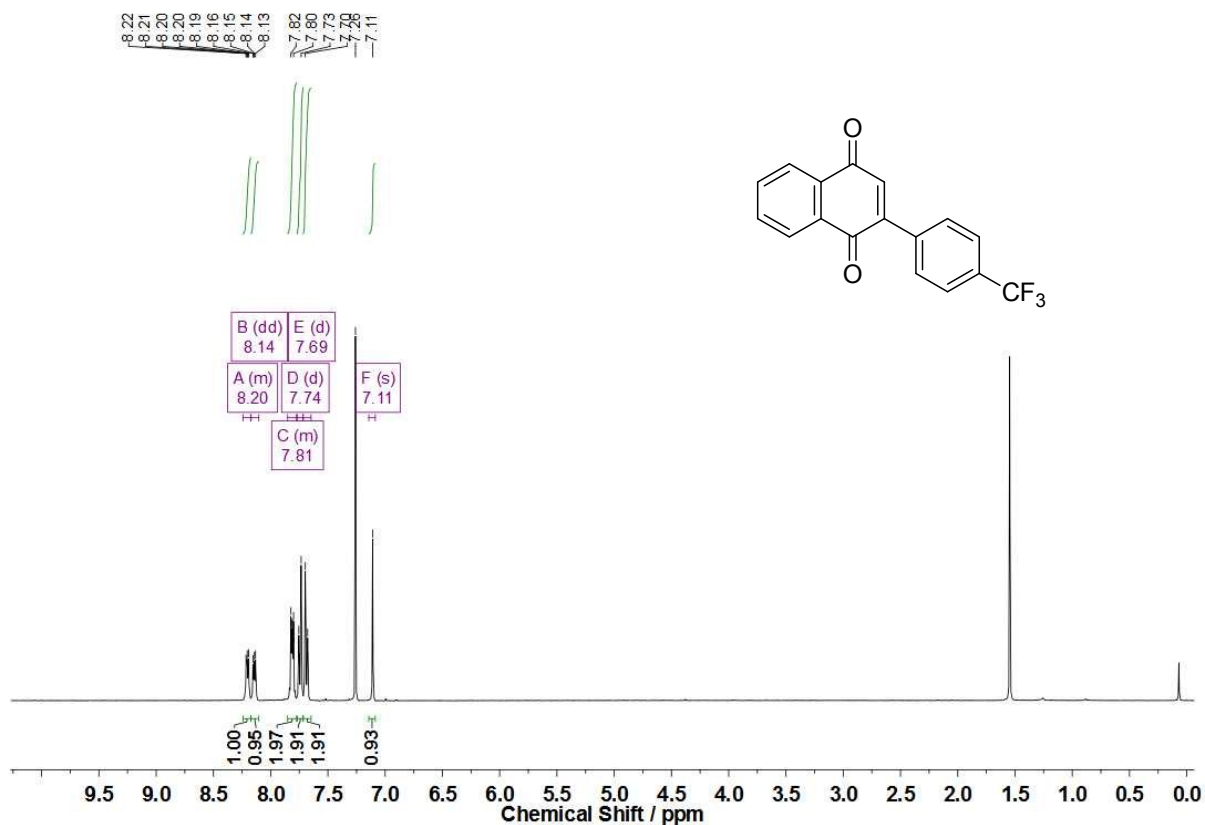
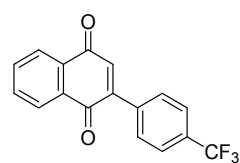


**Fig. S14**  $^1\text{H}$  NMR (400 MHz,  $\text{CDCl}_3$ ) spectrum of PNQ-7.

2-(4-Trifluoromethylphenyl)-1,4-naphthoquinone (PNQ-7)<sup>S1</sup>: A yellow solid purified by flash column chromatography (n-hexane: ethyl acetate = 20 : 1).  $R_f$  0.4 (n-hexane: ethyl acetate = 4 : 1).  $^1\text{H}$  NMR (400 MHz,  $\text{CDCl}_3$ )  $\delta_{\text{H}}$  8.24 – 8.17



(m, 1H), 8.14 (dd,  $J = 5.9, 3.1$  Hz, 1H), 7.85 – 7.77 (m, 2H), 7.74 (d,  $J = 8.2$  Hz, 2H), 7.69 (d,  $J = 8.3$  Hz, 2H), 7.11 (s, 1H).

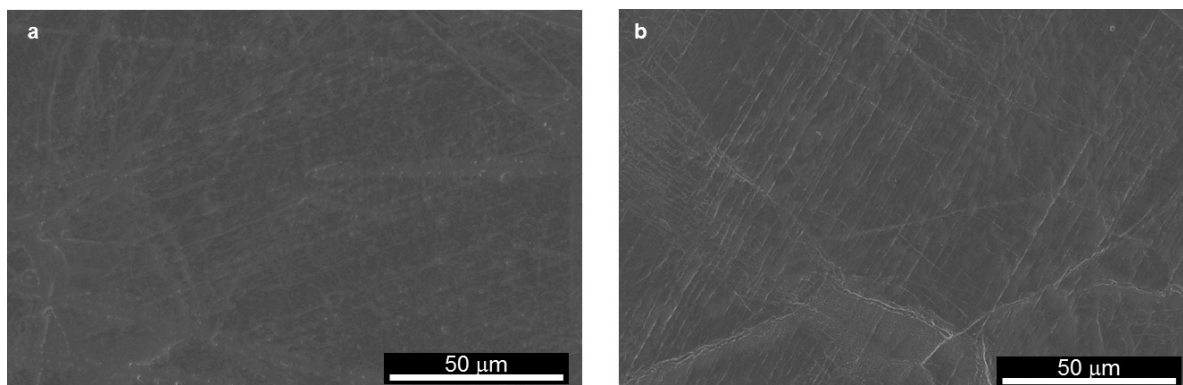


**Fig. S15** SEM images of lithium metal anodes for the (a) PNQ-4 and (b) PNQ-7 catholytes. Cell conditions: a high current rate of  $400 \text{ mA g}^{-1}$  after 100 cycles.

***Design of tubular flow batteries:*** The battery was fabricated in a dry room (see also Fig. S16). Lithium foil and copper mesh were combined by a roller and wound into a spiral shape. The twisted bundle of Li metal foil grafted on Cu mesh was wrapped by a PE separator. It was then wound by carbon cloth (1071 HCB, AvCarb) followed by aluminum mesh. This assembly was packaged using a heat shrinkable rubber tube. The catholyte (2.0 mL) was injected into the cell and both ends of each cell were sealed up using a glue gun and a glue-lined heat shrink tube. For the catholyte circulation, the tube cell was connected to an external tank (20 mL) and a circulation pump through Viton<sup>®</sup> tubing. Precyclings were performed for the tube system stabilization.

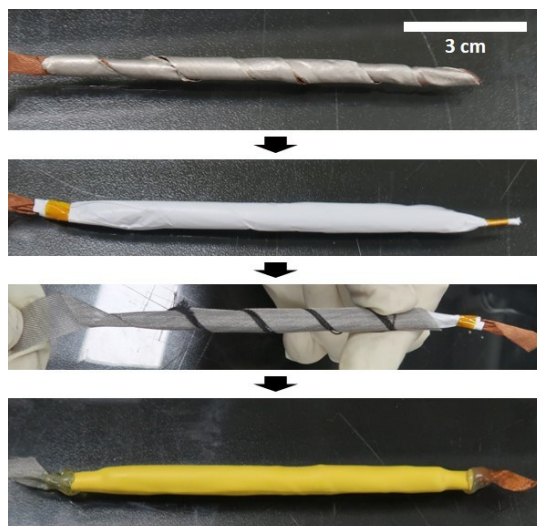


**Fig. S16** Fabrication steps for a tubular lithium-organic battery.

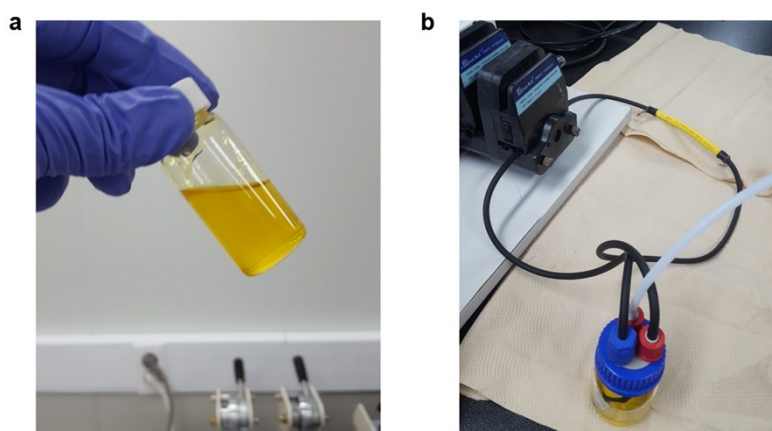


**Fig. S17** (a) Fully soluble state of the PNQ-1 catholyte (0.1 M) and (b) a tubular lithium-organic flow battery system with an external tank and a pump.

**Solubility test:** the solubility test was performed according to the method developed by the Chamberlain group.<sup>54</sup> Standard PNQ-1 samples within a concentration range from 20 to 200 mM were prepared (Table S1). And the saturated PNQ-1 solution was made by the addition of an excess amount of PNQ-1 in TEGDME (1 mL), followed by filtration. The above-mentioned samples (1  $\mu$ L) were diluted by pouring into a bare TEGDME solvent (5 mL). UV/Vis absorption spectra of the sample solutions were measured, and the maximum concentration of PNQ-1 was estimated to be 0.31 M from the calibration curve using the maximum absorbance at 249 nm (see also Fig. S18).

**Table S1.** UV/Vis absorption of the PNQ-1 solution

Concentration [mM]	Absorbance at 249 nm
20	0.037
50	0.072
100	0.136
200	0.353
Saturated state (max. solubility)	0.542

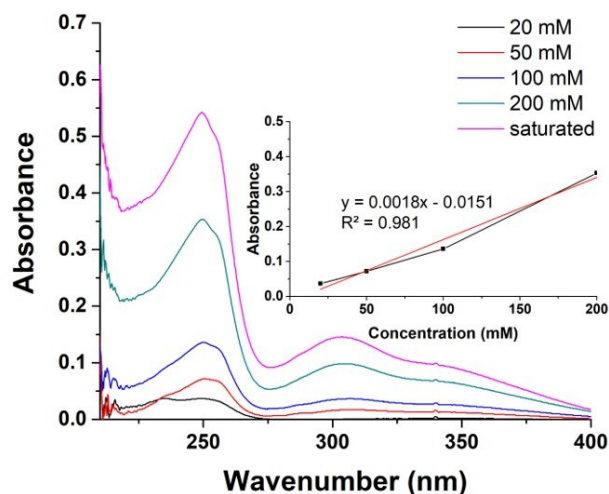


**Fig. S18** UV/Vis absorption spectra of PNQ-1; the inset indicates the corresponding calibration curve obtained at 249 nm.

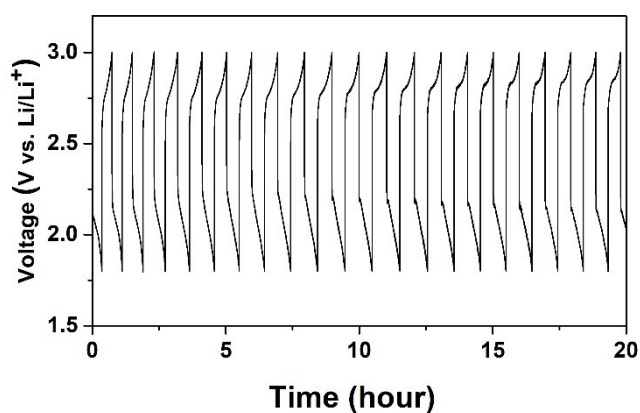


**Fig. S19** The charge–discharge cycle behavior of the tubular lithium-organic flow battery having the 0.1 M PNQ-1 catholyte.

***Fabrication of interdigitated back contact (IBC) crystalline silicon (c-Si) solar module:*** IBC c-Si solar cells were fabricated using n-type Czochralski (Cz) Si wafers with a resistivity of 1–3  $\Omega\text{cm}$  and a thickness of 200  $\mu\text{m}$ . The backside of each cell consisted of an interdigitated emitter and a back surface field (BSF) formed by the selective area diffusion of boron and phosphorus. The emitter and BSF were formed by diffusion process of boron and phosphorous using a spin-on-dopant method with B155 and P509 (Filmtronics), respectively. A 10 nm-thick  $\text{Al}_2\text{O}_3$  passivation layer was deposited on the front and rear side of the doped c-Si wafer via atomic layer deposition (Lucida D100, NCD). A 65 nm-thick  $\text{SiN}_x$  film was deposited using plasma-enhanced chemical vapor deposition (PE-CVD; PEH-600, SORONA) to form the anti-reflection layer. For the metal electrodes, interdigitated grid patterns were formed at the emitter/BSF regions by photolithography, and a 500 nm-thick Al film was thermally deposited. The IBC solar cells were isolated by a dicing process. To fabricate the solar module, IBC solar cells were arranged to connect the electrodes. A transparent UV-curable polymer (NOA 71, Norland Products, Inc.) was coated onto the front surface of the IBC solar cells and then fully cured by UV exposure for 300 s. A 500 nm-thick Al film was

thermally deposited through a shadow mask to interconnect the cells in series. The device area of the IBC solar module is 5.4 cm<sup>2</sup>. The IBC solar module was measured using a solar simulator (Class AAA, Oriel Sol3A, Newport) under AM 1.5G illumination. The incident flux was measured using a calibrated power meter and double-checked using an NREL-calibrated solar cell (PV Measurements, Inc.).

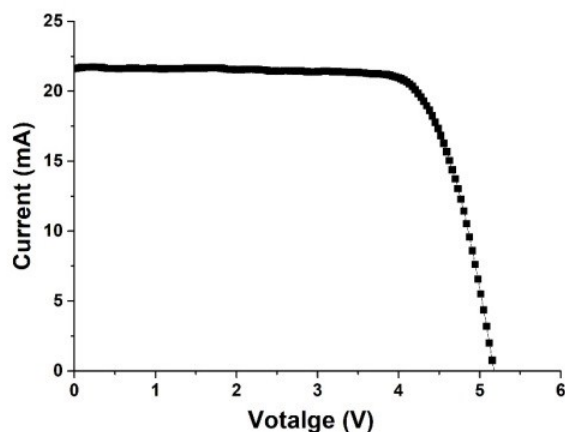
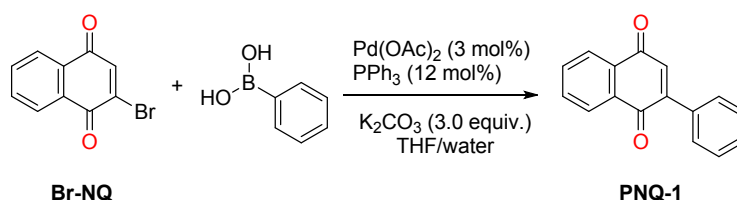


**Fig. S20** A photocurrent–voltage correlation of crystalline solar cell module.

**The cost calculation of PNQ-1:** The cost of the active materials is one of the critical factors along with their greenness, sustainability, and electrochemical performance to evaluate the practicality of rechargeable battery systems. Reagents, catalysts, and substrate precursors were purchased from the standard supplier (Sigma Aldrich) to prepare synthetic redox-active molecules.

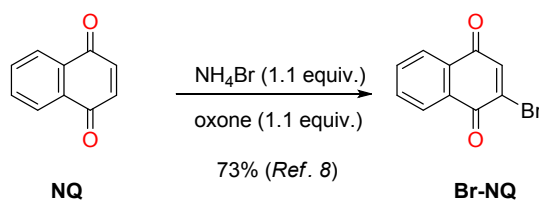


**Scheme S1.** The Pd-catalyzed Suzuki cross-coupling reaction to afford arylated PNQ-1.

Based on the Scheme S1, the cost of synthetic compounds has been estimated

- Commercial Br-NQ: 100 mg (0.42 mmol) 0.679 USD (67.90 \$/10 g; Catalogue # 510300)
- Pd(OAc)<sub>2</sub>: 3 mol% (2.84 mg) 0.126 USD (443.50 \$ /10 g; Catalogue # 205869)
- Phenylboronic acid: 1.5 equiv. (76.8 mg) 0.125 USD (81.30 \$ /50 g; Catalogue # P20009)
- PPh<sub>3</sub>: 12 mol% (13.28 mg) 0.003 USD (61.00 \$ /250 g; Catalogue # 93092)
- K<sub>2</sub>CO<sub>3</sub>: 3.0 equiv. (175 mg) 0.030 USD (94.00 \$ /500 g; Catalogue # P5833)
- Reaction yield: 86% (0.36 mmol; 84.33 mg) for PNQ-1
- 84.33 mg PNQ-1; Overall cost: 0.963 USD
- Thus, the estimated cost: ~11.4 USD / 1.0 g of PNQ-1

The key cost factor is the price of commercial Br-NQ. Yet, it can be also readily prepared from the cheaper NQ substrate by the oxidative bromination (see Scheme S2 below).<sup>55</sup> The total price will be significantly reduced to ~4.0 USD to yield 1.0 g of PNQ-1.



**Scheme S2.** Oxidative bromination to afford Br-NQ from NQ.

- NQ: 100 mg (0.63 mmol) 0.0349 USD (34.90 \$/100 g; Catalogue # 152757)
- Oxone: 1.1 equiv. (213 mg) 0.014 USD (68.00 \$/1 kg; Catalogue # 228036)
- NH<sub>4</sub>Br: 1.1 equiv. (68 mg) 0.013 USD (95.00 \$/500 g; Catalogue # 213349)
- Reaction yield: 73% (0.46 mmol; 109 mg) for Br-NQ
- The cost to produce synthetic Br-NQ: 100 mg; ~0.056 USD
- Thus, the estimated total cost: ~4.0 USD/ 1.0 g of PNQ-1

### III. References

- S1 M. T. Molina, C. Navarro, A. Moreno and A. G. Csáký, *Org. Lett.*, 2009, **11**, 4938–4941.
- S2 O. M. Demchuk and K. M. Pietrusiewicz, *Synlett*, 2009, **7**, 1149–1153.
- S3 M. L. N. Rao and S. Giri, *RSC Adv.*, 2012, **2**, 12739–12750.
- S4 J. Friedl, M. A. Lebedeva, K. Porfyrakis, U. Stimming and T. W. Chamberlain, *J. Am. Chem. Soc.*, 2018, **140**, 401–405.
- S5 M. A. Kumar, M. Naresh, C. N. Rohitha and N. Narender, *Synth. Commun.*, 2013, **43**, 3121–3129.